

3. G. A. Voropaev, "Calculation of certain characteristics of a turbulent boundary layer on a compliant surface," in: *Mathematical Methods of Studying Flow Hydrodynamics* [in Russian], Naukova Dumka, Kiev (1978), pp. 9-13.
4. K. K. Fedyaevskii, A. S. Ginevskii, and A. V. Kolesnikov, *Calculation of the Turbulent Boundary Layer of an Incompressible Fluid* [in Russian], Sudostroenie, Leningrad (1973).
5. W. B. Nicoll, A. B. Strong, and K. A. Woolner, "On the laminar motion of a fluid near an oscillating porous infinite plane," *Trans. ASME, Ser. E*, 35, No. 1, 324-327 (1968).
6. A. B. Airapetov, "Laminar motion of a viscous incompressible fluid next to a permeable cylinder vibrating in the fluid," *Uch. Zap. TsAGI*, 4, No. 5, 88-92 (1973).
7. K. R. Sreenivasan and R. A. Antonia, "Properties of wall shear stress fluctuations in a turbulent duct flow," *Trans. ASME, Ser. E*, 44, No. 3, 389-395 (1977).
8. B. M. Efimtsov and S. E. Shubin, "Probability characteristics of pressure pulsations in a boundary layer on the surface of an aircraft," in: *Aeronautical Acoustics*, Tr. TsAGI, No. 1655 (1975), pp. 3-14.
9. P. M. Ogivalov, N. I. Malinin, V. P. Netrobenko, and B. P. Kishkin, *Structural Polymers* [in Russian], Vol. 1, Moscow State Univ. (1972).

NUMERICAL SOLUTION OF A TWO-DIMENSIONAL PROBLEM OF THE TRANSIENT
HYDRODYNAMICS OF A COMPRESSIBLE NON-NEWTONIAN FLUID

S. D. Tseitlin

UDC 532.135

A solution is presented for a transient two-dimensional problem of the hydrodynamics of a compressible non-Newtonian fluid connected with the propagation and damping of shock waves in a well.

The physical processes connected with well drilling have been studied in increasing detail in recent times, a fact related to the seriousness of the consequences of emergency situations at oil and gas extraction sites. Theoretical study of the hydrodynamics of wells is complicated by the need to solve problems for non-Newtonian fluids — which includes most drilling fluids. Here, most of the work that has been done has examined unidimensional and quasi-unidimensional hydrodynamic problems, with investigators neglecting or averaging two-dimensional and nonlinear effects [1, 2].

Examined below is a two-dimensional transient problem of the hydrodynamics of a compressible non-Newtonian fluid with allowance for several nonlinear phenomena which might exert a marked effect in the generation and propagation of shock waves in long channels. We chose for the form of the rheological equation a relation describing shear stress as an exponential function of shear rate, which is a good approximation for most drilling fluids.

Given this model, we may study a whole range of problems of dynamics connected with the opening up of beds with pressure anomalies, the closing of pipe connections, start-up of pumps, lowering and raising of drilling equipment, etc. Here, we examine the first of these problems and solve it by the method of fractional steps [3] on an R-1040 computer.

The unsteady motion of a non-Newtonian fluid is described by the following dynamic equation [4, 5]:

$$\rho \frac{\partial \mathbf{v}}{\partial t} + \rho \nabla \mathbf{v} \cdot \mathbf{v} = -\nabla P + \operatorname{div} \bar{\tau} + \rho \mathbf{g}. \quad (1)$$

In the case of a compressible fluid, apart from the shear stresses, the viscous stress tensor should also account for linear strain [4], i.e.,

Central Geophysical Department of the Ministry of the Petroleum Industry, Moscow.
Translated from *Inzhenerno-Fizicheskii Zhurnal*, Vol. 40, No. 4, pp. 664-672, April, 1981.
Original article submitted March 10, 1980.

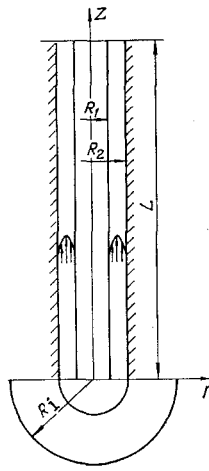


Fig. 1. General view of channel geometry.

$$\bar{\tau} = \bar{\tau}' + \frac{2}{3} \eta (\operatorname{div} \mathbf{v}) \delta. \quad (2)$$

We assume that for the fluid in question there is assigned a nonlinear rheological equation of state which provides for agreement between $\bar{\tau}$ and the tension tensor (\bar{D}). Here, $\bar{\tau}' = \bar{\tau}$, since the liquid was assumed to have been incompressible ($\operatorname{div} \mathbf{v} = 0$) in deriving the rheological equation

$$\bar{\tau}' = g(\bar{D}),$$

where $\bar{D} = \frac{1}{2} (\nabla \mathbf{v} + \nabla \mathbf{v}^T)$. The specific form of this relation for the so-called generalized non-Newtonian fluid [4] is expressed in terms of the second principal invariant of the tensor

$$\bar{\tau}' = 2\eta(S)\bar{D}, \quad (3)$$

where $S = 2\operatorname{tr}(\bar{D}^2)$, here tr is the trace of the tensor.

The value of η is assumed constant for a Newtonian fluid, and Eq. (1) converts to the Navier-Stokes equation. Substitution of Eq. (2) into (1) with allowance for (3) leads to the generalized form of the Navier-Stokes equation [4, 5]:

$$\rho \frac{\partial \mathbf{v}}{\partial t} + \rho \nabla \mathbf{v} \cdot \mathbf{v} = -\nabla P + \rho \mathbf{g} + \eta(S) \left\{ \nabla^2 \mathbf{v} + \frac{1}{3} \operatorname{grad} \operatorname{div} \mathbf{v} \right\} + 2\bar{D} \operatorname{grad} \eta(S) - \frac{2}{3} \operatorname{grad} \eta(S) \operatorname{div} \mathbf{v}. \quad (4)$$

Equation (4) will be integrated with a power law of change in viscosity [4], i.e., where

$$\eta(S) = kS^{(n-1)/2}. \quad (5)$$

We should note that drilling fluids are described well by relations of the type (5) for $n < 1$. To close the system, together with Eqs. (4) and (5), we should examine the equation of continuity for a compressible fluid [4]:

$$-\frac{\partial P}{\partial t} = \rho c^2 \operatorname{div} \mathbf{v}, \quad (6)$$

where $c = \sqrt{k_h/\rho}$.

Let us now examine the following problem. Let a viscous fluid with a known rheology enter the bottom of a vertical tube (Fig. 1) of length L with an annular cross section of radii R_1 and R_2 (in particular, the internal radius can be $R_1 = 0$). A steady flow is established in the tube with a profile which depends on the type of rheological law, the geometry of the channel, and the mass flow rate [1]. We will study the propagation of dynamic perturbations which arise with an abrupt change in the mass flow rate or the pressure at the ends of the channel in the case of the movement of a non-Newtonian fluid in the channel.

Let us choose a cylindrical system of coordinates, (z, φ, r) , with the z axis coinciding

with the axis of the channel and the origin located on the bottom cross section. Considering that the velocity \mathbf{v} has only a z -th component $v_z = v(r, z)$, we may specify the form of the tension tensor and S , as well as the form of Eq. (3). In a cylindrical coordinate system, the tension tensor has the form

$$D = \begin{pmatrix} \frac{\partial v_z}{\partial z} & \frac{1}{2} \left(\frac{\partial v_z}{\partial r} + \frac{\partial v_r}{\partial z} \right) \\ \frac{1}{2} \left(\frac{\partial v_z}{\partial r} + \frac{\partial v_r}{\partial z} \right) & \frac{\partial v_r}{\partial r} \\ \frac{1}{2} \left(\frac{\partial v_\varphi}{\partial z} + \frac{1}{r} \frac{\partial v_z}{\partial \varphi} \right) & \frac{1}{2} \left(\frac{1}{r} \frac{\partial v_r}{\partial \varphi} + \frac{\partial v_\varphi}{\partial r} - \frac{v_\varphi}{r} \right) \\ & \frac{1}{2} \left(\frac{\partial v_\varphi}{\partial z} + \frac{1}{r} \frac{\partial v_z}{\partial \varphi} \right) \\ & \frac{1}{2} \left(\frac{1}{r} \frac{\partial v_r}{\partial \varphi} + \frac{\partial v_\varphi}{\partial r} - \frac{v_\varphi}{r} \right) \\ & \frac{1}{r} \left(\frac{\partial v_\varphi}{\partial \varphi} + v_r \right) \end{pmatrix}; \quad (7)$$

thus in our case

$$S = 2\text{tr}(D^2) = 2 \left(\frac{\partial v}{\partial z} \right)^2 + \left(\frac{\partial v}{\partial r} \right)^2. \quad (8)$$

The system of equations (4)-(6) takes the form

$$\rho \frac{\partial v}{\partial t} + \rho v \frac{\partial v}{\partial z} = - \frac{\partial P}{\partial z} + \rho g + \eta \left(\frac{4}{3} \frac{\partial^2 v}{\partial z^2} + \frac{\partial^2 v}{\partial r^2} + \frac{1}{r} \frac{\partial v}{\partial r} \right) + \frac{4}{3} \frac{\partial v}{\partial z} \frac{\partial \eta}{\partial z} + \frac{\partial v}{\partial r} \frac{\partial \eta}{\partial r},$$

$$\frac{\partial P}{\partial t} = -c^2 \rho \frac{\partial v}{\partial z},$$

$$\eta = k \left\{ \left(\frac{\partial v}{\partial r} \right)^2 + 2 \left(\frac{\partial v}{\partial z} \right)^2 \right\}^{\frac{n-1}{2}}; \quad \rho = \rho_0 \left(1 + \frac{P - P_0}{k_h} \right). \quad (9)$$

The values of k and n are considered known, and are taken from an empirical flow curve.

The channel is assumed to be isothermal. Flow is laminar in character everywhere in the channel. In the case of steady flow, most of the terms of Eqs. (9) vanish, and the solution can be written in the form of a quadrature [1]. This solution will be taken for the initial distribution of the parameters in the channel ($t < 0$). The boundary conditions may differ, depending on the type of flow perturbation.

In the present work, we investigated the dynamics of the opening of a bed with a pressure anomaly, and chose the following boundary conditions. On the wells we assigned the condition of adhesion $v(r = R_1) = v(r = R_2) = 0$, $\partial P / \partial r = 0$. At the channel outlet we assigned a constant pressure $P(z = L) = \text{const} = 1 \text{ atm}$. The boundary condition at the bottom of the channel ($z = 0$) was assigned on the basis of the following assumptions. Let a gas bed of infinite thickness be opened at the moment of time $t = 0$ with a large increase in pressure over $P_b(z = 0, t < 0)$. In emergency situations, the magnitude of the anomalous pressure in the bed $P_k = \rho_i - \rho g L$ may reach several tens or even hundreds of atmospheres. A gas flow $Q(t)$ begins to enter the channel at $t > 0$, the magnitude of the flow being determined by the porosity and permeability of the reservoir (m and k_p , respectively), the viscosity of the gas μ , and the difference between the anomalous pressure of the bed and the pressure at the bottom of the borehole ($P_i - P_b(z = 0, t)$). From the theory of transient unidimensional filtration and with allowance for well imperfection in the assumption of quasistationariness, we may obtain the following to express the dependence of this flow on the above-noted parameters [2]

$$Q(t) = \frac{2\pi k_p R_2}{\mu} (P_i - P_b(t)) \exp\left(-\frac{R_2^2}{4\kappa t}\right), \quad (10)$$

where $\kappa = (k_p P_k) / (m\mu)$ is the coefficient of piezoconductivity.

Analysis of the steady-state velocity (the value of κ) for characteristic types of reservoirs shows that the process of establishing steady-state conditions takes place considerably more rapidly than does the change in pressure at the bottom of the borehole $P_b(t)$, i.e., the condition of quasistationariness, assumed in obtaining Eq. (10), is well satisfied at channel lengths $L \geq 50$ m. Since the volume of the gas entering the channel during this process is much less than the total volume of fluid in the channel, we can ignore the effect of the gas layer at the bottom of the well on the overall pattern of flow dynamics.

Thus, the boundary condition in the bottom section of the channel is assigned in the form of a dependence of velocity $v(z = 0, t)$ or flow rate on pressure obtained from Eq. (10). The initial velocity profile ($v(r, z)$ at $t \leq 0$) corresponds to steady-state flow of the fluid in a channel of the given configuration. At the channel outlet we assign the condition of the free surface $\frac{\partial v}{\partial z}(z = L) = 0$.

It is usual in studying shock waves in a fluid in tubes to ignore the nonlinear terms $v \frac{\partial v}{\partial z}$ and $\frac{\partial}{\partial z} \left(\eta \frac{\partial v}{\partial z} \right)$, which are indeed of lesser magnitude than the other terms in Eq. (9). However, since the channel length reaches several kilometers, these phenomena may have a marked effect on wave attenuation along the channel.

Having chosen characteristic values of time t_0 , length l_0 , viscosity η_0 , and pressure P_0 and converting to dimensionless quantities, we can rewrite system (9) in the form

$$\begin{aligned} \frac{\partial v}{\partial t} &= -v \frac{\partial v}{\partial z} - \frac{1}{Fr} + \frac{1}{Re} \left[\frac{4}{3} \frac{\partial}{\partial z} \left(\eta \frac{\partial v}{\partial z} \right) + \frac{1}{r} \frac{\partial}{\partial r} \left(r\eta \frac{\partial v}{\partial r} \right) \right] - Er \frac{\partial P}{\partial z}, \\ \frac{\partial P}{\partial t} &= -Er_p \frac{\partial v}{\partial z}, \\ \eta &= k \left\{ \left(\frac{\partial v}{\partial r} \right)^2 + 2 \left(\frac{\partial v}{\partial z} \right)^2 \right\}^{(n-1)/2}, \end{aligned} \quad (11)$$

where

$$Fr = \frac{v_0}{l_0 g}; \quad Re = \frac{l_0 v_0 \rho}{\eta_0}; \quad Er = \frac{P_0}{\rho v_0^2}; \quad Er_p = \frac{c^2 \rho}{P_0}.$$

For the numerical algorithm, we chose the method of fractional steps — specifically, the Douglas-Rachford scheme [3]. Let us write Eq. (10) in vector form

$$\frac{\partial X}{\partial t} = \Lambda X + Q,$$

where

$$X = \begin{pmatrix} v \\ P \end{pmatrix}; \quad \Lambda = \begin{pmatrix} -v \frac{\partial}{\partial z} + \frac{1}{Re} \left[\frac{4}{3} \frac{\partial}{\partial z} \left(\eta \frac{\partial}{\partial z} \right) + \frac{1}{r} \frac{\partial}{\partial r} \left(r\eta \frac{\partial}{\partial r} \right) \right] - Er \frac{\partial}{\partial z} \\ -Er_p \frac{\partial}{\partial z} \end{pmatrix}; \quad Q = \begin{pmatrix} g \\ 0 \end{pmatrix}.$$

We will represent the operator Λ in this equation in the form of the sum $\Lambda = \Lambda_z + \Lambda_r$, where

$$\begin{aligned} \Lambda_z &= \begin{pmatrix} -v \frac{\partial}{\partial z} + \frac{4}{3} \frac{1}{Re} \frac{\partial}{\partial z} \left(\eta \frac{\partial}{\partial z} \right) & -Er \frac{\partial}{\partial z} \\ -Er_p \frac{\partial}{\partial z} & 0 \end{pmatrix}; \\ \Lambda_r &= \begin{pmatrix} \frac{1}{Re} \frac{1}{r} \frac{\partial}{\partial r} \left(r\eta \frac{\partial}{\partial r} \right) & 0 \\ 0 & 0 \end{pmatrix}. \end{aligned}$$

Then, having chosen a grid with spatial steps h_r , h_z and the time step τ ($\omega = h_r \times h_z \times \tau$), we approximate the differential operators with the finite-difference operators ($\Lambda_r \sim \tilde{\Lambda}_r$, $\Lambda_z \sim \tilde{\Lambda}_z$), so that we obtain the following algebraic system:

$$\begin{aligned} \frac{X^{m+\frac{1}{2}} - X^m}{\tau} &= \tilde{\Lambda}_r X^{m+\frac{1}{2}} + \tilde{\Lambda}_z X^m, \\ \frac{X^{m+1} - X^{m+\frac{1}{2}}}{\tau} &= \tilde{\Lambda}_z X^{m+1} - \tilde{\Lambda}_r X^m \end{aligned} \quad (12)$$

(the superscript m indicates the number of the time layer ($t = m\tau$)).

The Douglas-Rachford scheme is known to be stable [3] and has an approximation in the case of linearity of Λ_r and Λ_z $O(|h|^2 + \tau)$. These operators are nonlinear in our case, although the numerical experiment showed that we could expect the same order of accuracy.

Each of the above operators, by virtue of their nonlinearity, depend on the sought functions (P and v). In the numerical solution of system (12), this dependence was accounted for by the usual method of displacing the time by $\tau/2$. Such an approach imposes additional conditions on the selection of a time step since it introduces an additional error into the solution, and is determined experimentally.

The system of algebraic equations (12) may be reduced to the following form:

$$\begin{aligned} A_1^m X_{i-1j}^{m+\frac{1}{2}} - (A_2^m + E) X_{ij}^{m+\frac{1}{2}} + A_3^m X_{i+1j}^{m+\frac{1}{2}} &= -EX_{ij}^m - \tau \tilde{\Lambda}_z^m X_{ij}^m, \\ B_1^{m+\frac{1}{2}} X_{ij-1}^{m+1} - (B_2^{m+\frac{1}{2}} + E) X_{ij}^{m+1} + B_3^{m+\frac{1}{2}} X_{ij+1}^{m+1} &= -EX_{ij}^{m+\frac{1}{2}} + \tau \tilde{\Lambda}_r^m X_{ij}^m, \end{aligned} \quad (13)$$

where A_1^m , A_2^m , A_3^m , $B_1^{m+\frac{1}{2}}$, $B_2^{m+\frac{1}{2}}$, $B_3^{m+\frac{1}{2}}$ are square matrices (of the second rank) obtained in approximating the initial equations by finite-difference equations; E is the unit matrix.

System of equations (13), with the corresponding boundary and initial conditions, was solved by means of a matrix trial run [3]. We selected an 8×100 grid with a time step $\tau = 3 \cdot 10^{-9}$ sec. Here, 1 sec of real time required about 10 min of machine computation on the R-1040 computer.

Let us examine a typical example of transient flow of a drilling fluid in the annular space (between the casing and tubing of the drill pipe) (Fig. 1). The radii of the casing and tubing was chosen as $R_1 = 0.0735$ m and $R_2 = 0.1145$ m. The channel length was $L = 500$ m. The rheological characteristic of the fluid was assigned in the form of a power law with the indices $n = 0.5$; $k = 0.22$, i.e., $\tau = 0.22 \cdot S^{0.5/2}$. The top end of the drill pipe was assumed to be open, and at its surface we assigned the condition $P(z = L) = P_0 = 10^5$ N/m². We assigned a condition of adhesion on the channel walls, i.e., $v(r = R_1) = v(r = R_2) = 0$. At $t < 0$, we assumed a non-Newtonian fluid flowed in the channel with a velocity and pressure distribution corresponding to the steady state [1].

At $t \geq 0$, an anomalous-pressure bed was opened and there was an associated abrupt increase in pressure and flow rate at the lower end of the pipe ($z = 0$). The front and amplitude of the increase in pressure were assumed to be connected by Eq. (10). Calculations were performed for $P_n = 10^7$ N/m² + ρgL ; $\mu = 10^{-4}$ N·sec/m²; $k_p = (0.1-1)D$; $m = 0.2$; $Q_0 = 25 \cdot 10^{-3}$ m³/sec.

Let us examine and discuss certain of the results obtained.

1. Figure 2 shows the changes in pressure and flow rate (or velocity) at the bottom of the borehole ($z = 0$) in relation to time. In the first $\sim 3 \cdot 10^{-2}$ sec, pressure and flow rate are established at certain constant values $P = 46 \cdot 10^5$ N/m² + ρgL and $Q = 72 \cdot 10^{-3}$ m³/sec, with both the front and the amplitude of these quantities being dependent on the properties of the bed and the channel. After a time roughly equal to $\sim T^0 = \frac{2L}{c} \approx 77 \cdot 10^{-2}$ sec, a rarefaction wave reflected from the free surface arrives. This wave is weakened considerably as a result of

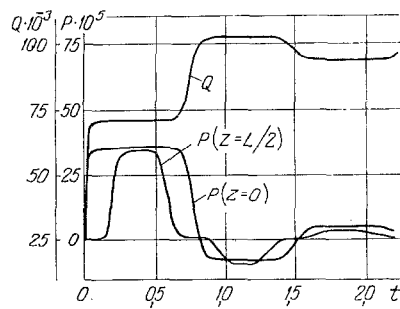


Fig. 2

Fig. 2. Change in pressure (P , N/m^2) and flow rate (Q , m^3/sec) at the bottom of the well ($z = 0$) and the change in pressure in the middle of the channel ($z = L/2$) in relation to time t , sec.

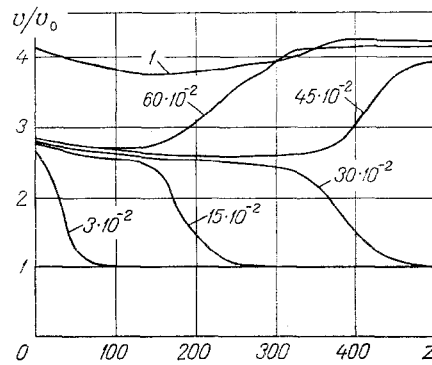


Fig. 3

Fig. 3. Relative change in velocity along channel $v/v_0 = f(z)$ at different moments of time (numbers next to curves denote the time in seconds). z , m.

dissipation during its movement up and down the channel. The arrival of the rarefaction wave establishes some new value of pressure at the bottom which is less than the initial hydrostatic pressure. Here, in view of (10), there is some increase in the flow rate (from 72 to $102 \cdot 10^{-3} m^3/sec$), i.e., an interesting phenomenon occurs in the dynamics of opening an anomalous-pressure bed whereby the arrival of a rarefaction wave from the initial shock causes additional gas to be sucked out of the bed. The intensity of this phenomenon depends on the viscosity of the drilling fluid, the geometry of the channel, and the properties of the reservoir, and it may prove decisive in subsequent transfer of gas from the bed. After a time of $2T_0$, the next wave reflected from the surface arrives. It is even more weakened than the preceding wave, with diffuse fronts. The arrival of this wave causes a certain increase in pressure at the bottom and, thus, a decrease in the rate of flow from the bed. This process rapidly dies out, and after several seconds ($\sim 3-5$) nearly steady-state flow has been established in the channel, with new values of pressure and flow rate at the bottom.

Figure 2 also shows a curve depicting the change in pressure in the middle of the channel ($z = L/2$). It is apparent here that there is a gradual diffusion of the fronts and a reduction in the amplitudes of the pressure pulses over time. The shift in the pressure curve over time is explained by the shift in the observation point along the channel by the amount $z = L/2$. We should note that the shape of the pressure pulse here differs markedly from the shape of the pressure pulse at the bottom. This agrees well with the physics of the phenomenon and experimental findings.

2. Figure 3 shows the change in pressure along the channel for different moments of time. It is apparent how the velocity changes along the channel, in which there was initially a steady-state flow with a certain constant velocity corresponding to the flow rate ($Q_0 = 25 \cdot 10^{-3} m^3/sec$). Since the velocity is different at different points of the channel radius, Fig. 3 also shows the change in velocity approximately in the middle of the channel (at $r = (R_1 + R_2)/2$). The velocity change at other points of the channel cross section is similar in nature.

The initial moment of bed opening is accompanied by a rapid increase in velocity in the bottom zone, while velocity remains equal to the initial value in most of the channel. There is then a gradual increase in velocity along the channel with parallel development of the front. At a time $t = L/c$, roughly the same velocity is established throughout the channel; this velocity at the open end of the pipe then begins to increase simultaneous with the formation of a reflected wave. The latter, increasingly diffuse and attenuating, travels toward the bottom. We should note that if the damping associated with the viscosity of the fluid and friction against the channel wall were absent, the initial velocity at the free surface would be doubled. In our formulation, however, processes connected with attenuation of the wave along the channel are considered, so that the increase in velocity at $z = L$ is appreciably lower.

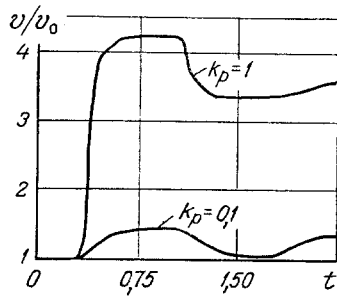


Fig. 4. Relative change in velocity (v/v_0) at the top of the well ($z = L$) in relation to time (t , sec) for two values of bed permeability coefficient (k_p, D).

There is an additional change in flow rate and velocity with the arrival of the rarefaction wave at the bottom (at $t > T_0$) and a new perturbation is directed along the channel. The waves that are generated meet one another, are diffracted, and attenuate until a certain new constant steady-state flow is established along the entire length of the channel. This whole dynamic pattern depends on the geometry of the channel, the properties of the fluid, and the intensity of the perturbation — which in turn depends on the properties of the bed.

3. Figure 4 shows the relative change in velocity v/v_0 (or flow rate Q/Q_0) in the top section of the pipe obtained from a solution of the problem relative to time for two values of permeability coefficient ($k_p = 1D$ and $k_p = 0.2D$). It is apparent how bed permeability affects the velocity magnitude and front. Allowing for the effect of viscosity along the channel makes it possible to determine the attenuation dynamics as a function of the chosen parameters of our model. The curves in Fig. 4 are also interesting in that they represent values which might (and should) be measured in the top section of the channel and by which a judgment can be made as to the degree and force of the gas release.

4. We should note one other important result obtained from the solution of the two-dimensional transient problem. In those parts of the channel where the flow is quasi-stationary at a given moment of time, i.e., where $\partial v/\partial t$ and $\partial v/\partial z$ are small, the velocity profile is close in form to the profile corresponding to stationary flow. However, in those parts of the channel where the change in velocity along the channel is substantial (see Fig. 3), the form of the profile changes appreciably. Here, there is a corresponding increase in the resistance to the flow in the pipe, which is consistent with the physics of the phenomenon. Thus, in our example (where $k_p = 1D$), the velocity in the region of the shock front in the boundary layer is 38% higher than it should be at the given flow rate in the steady-state case.

Thus, with the appearance of a shock wave, there is a marked change in the flow profile and an increase in the degree of attenuation in the channel.

In conclusion, we should note that the well hydrodynamic model obtained here, taking into account the non-Newtonian properties of drilling fluids, makes it possible to conduct broad numerical experiments to study the physical processes connected with well dynamics.

NOTATION

ρ , density of fluid; v , fluid velocity vector; P , pressure; $\bar{\tau}^T$, viscous shear stress tensor; g , acceleration due to gravity; $\bar{\tau}$, viscous stress tensor; η , dynamic viscosity coefficient; δ , Kronecker symbol; \bar{D} , shear rate tensor; v^T , transformed velocity vector; S , invariant of shear rate tensor; n , exponent of power rheological law; k , constant of power rheological law; c , speed of sound in an elastic fluid; k_H , bulk modulus of elasticity; L , length of channel; R_1 , internal radius of annular space; R_2 , external radius of annular space; ρ_0 , density of fluid at atmospheric pressure P_0 ; P_b , pressure at the bottom of the borehole; P_i , initial pressure in the gas bed (at $t \leq 0$); $Q(t)$, flow rate of fluid; k_p , permeability of reservoir; μ , dynamic viscosity coefficient of the gas; $\Lambda, \Lambda_r, \Lambda_z$, differential operators; τ , time step; h_r, h_z , spatial steps; $\tilde{\Lambda}_r, \tilde{\Lambda}_z$, finite-difference operators.

LITERATURE CITED

1. U. L. Wilkinson, Non-Newtonian Fluids [Russian translation], Mir, Moscow (1964).
2. I. A. Charnyi, Principles of Subsurface Hydraulics [in Russian], Gostoptekhizdat, Moscow (1956).
3. A. A. Samarskii, Introduction to the Theory of Difference Methods [in Russian], Nauka, Moscow (1971).
4. G. Astarita and G. Marrucci, Principles of Non-Newtonian Mechanics, McGraw-Hill (1974).
5. A. V. Lykov, Heat Exchange [in Russian], Énergiya, Moscow (1972).

STABILITY OF A CONVECTIVE FLOW OF A VISCOUS FLUID BY THE METHOD OF LOCAL POTENTIAL

V. V. Gorlei and V. A. Shenderovskii

UDC 532.516

A study is made of the stability of convective fluid flow caused by an external temperature gradient and heat sources uniformly distributed in the fluid.

Interest has recently been increasing in the study of convective fluid flow caused by internal heat sources. The physical mechanism of heat liberation may vary in different cases: Joulian dissipation, radiant heat transfer, absorption of external radiation, etc. Together with this, the results in [1, 2] showed the destabilizing effect of viscosity non-uniformity. It is naturally of interest to investigate the stability of convective motion caused both by an external temperature gradient and internal heat liberation in considering the temperature dependence of viscosity. For this purpose, we will examine the convective flow of a viscous fluid in a long vertical layer bounded by parallel surfaces $x = \pm d$ maintained at fixed temperatures $T = \pm \theta$. Let internal heat sources with a constant volume density q be uniformly distributed throughout the volume of the liquid. We will assume that the viscosity of the liquid depends on the temperature according to the linear law

$$\nu = \nu_0(1 - \alpha T), \quad (1)$$

where ν_0 is the maximum value of viscosity reached on the cold ($T = -\theta$) surface; α , temperature coefficient.

We will adopt the variational approach to study the stability of the convective flow — specifically, the method of local potential. We will construct a functional having certain extreme properties and dependent on two types of variables [3]. In accordance with [4], we will proceed on the basis of linearized equations of a perturbed state [1]

$$\frac{\partial u'_x}{\partial t} + G \bar{u}_z \frac{\partial u'_x}{\partial z} = - \frac{\partial p'}{\partial x} + \bar{\eta} \left(\frac{\partial^2}{\partial x^2} + \frac{\partial^2}{\partial z^2} \right) u'_x + 2 \frac{\partial \bar{\eta}}{\partial x} \frac{\partial u'_x}{\partial x} + \frac{\partial \eta'}{\partial z} \frac{\partial \bar{u}_z}{\partial x}, \quad (2)$$

$$\frac{\partial u'_z}{\partial t} + G \left[\bar{u}_z \frac{\partial u'_z}{\partial z} + u'_x \frac{\partial \bar{u}_z}{\partial x} \right] = - \frac{\partial p'}{\partial z} + \bar{\eta} \left(\frac{\partial^2}{\partial x^2} + \frac{\partial^2}{\partial z^2} \right) u'_z + \eta' \frac{\partial^2 \bar{u}_z}{\partial x^2} + \frac{\partial \bar{\eta}}{\partial x} \frac{\partial u'_z}{\partial x} + \frac{\partial \eta'}{\partial x} \frac{\partial \bar{u}_z}{\partial x} + \frac{\partial \bar{\eta}}{\partial x} \frac{\partial u'_x}{\partial z} + T', \quad (3)$$

$$\frac{\partial T'}{\partial t} + G \left[u'_x \frac{\partial \bar{T}}{\partial x} + \bar{u}_z \frac{\partial T'}{\partial z} \right] = \frac{1}{Pr} \left(\frac{\partial^2}{\partial x^2} + \frac{\partial^2}{\partial z^2} \right) T', \quad (4)$$

$$G = g\beta q d^5 / 2\nu_0^2 \rho c_p \chi; \quad Pr = \nu_0 / \chi; \quad \gamma = \alpha q d^2 / 2\rho c_p \chi; \quad \eta = 1 - \gamma T$$

with the boundary conditions

$$\bar{u}_z(\pm 1) = 0, \quad \bar{T}(\pm 1) = N, \quad u'_x(\pm 1) = u'_z(\pm 1) = T'(\pm 1) = 0.$$

Here the units of distance, time, velocity, temperature, and pressure are, respectively: d ; d^2/ν_0 ; $g\beta q d^4 / 2\nu_0 \rho c_p \chi$; $q d^2 / 2\rho c_p \chi$; $g\beta q d^3 / 2c_p \chi$; $N = G_\theta / G$, where $G_\theta = g\beta \theta d^3 / \nu_0^2$; u_x, u_z , projections of the perturbed velocities on the x and z axes; p', T' , pressure and temperature perturbations; \bar{T} and \bar{u}_z , their mean values. Having performed all mathematical operations similar to the

Chernovtsy State University. Translated from *Inzhernerno-Fizicheskii Zhurnal*, Vol. 40, No. 4, pp. 673-677, April, 1981. Original article submitted March 23, 1980.